A Novel Gradual Faults Diagnosis Using The Photovoltaic Plant Reflectometry Profile

Najwa Lamdihine, Mohamed Ouassaid, Ghassane Aniba

Engineering for Smart & Sustainable Systems Research Center
Mohammadia School of Engineers (EMI), Mohamed V University in Rabat, Morocco
najwa.lamdihine@research.emi.ac.ma,{ouassaid,ghassane}@emi.ac.ma

***Abstract*—This paper presents a novel gradual defects diagnosis technique for photovoltaic (PV) panels using a new concept named the photovoltaic plant reflectometry profile (PPRP). In fact, the maintaining of the good functioning of PV systems requires a highly accurate diagnosis for detecting defects not only at the begining, during the commissioning of the PV systems, but also throughout their lifetime. The proposed technique in this paper allows not only the detection of a discordance between the datasheet and the measured performance of the manufactured PV panels, but also to find the exact location of the defective one on an already installed PV plant. The PPRP is a new analytical model and criterion used to compare between the reflected signal that is received within the PV Plant after its transmission and the ideal (expected) one computed analytically using the datasheet. Simulations were conducted using MATLAB Simulink to emulate the discordance between the ideal PPRP and the measured PPRP on the PV plant, and show precisely the expected location of the faulty module.**

***Index Terms*—Fault diagnosis, Photovoltaic systems, Reflectometry, Transmission lines.**

I. Introduction

THE desire to replace the fossil energies with clean and non-polluting renewable energies such as wind energy, biomass, hydro-energy, solar photovoltaic (PV), and in order to reduce greenhouse gas emissions gives an explanation for the extraordinary growth in the usage of PV plants all over the world. However, those plants as any system may fail because of electrical defects that may arise in them. In fact, the most serious PV failures can be categorized on three groups: electrical failures, such as open-circuit, short-circuit, ground fault, line-to-line fault and arc fault; thermal failures including hot spot formation and heating cables, and visual failures such as dust or soil formation, shading. Actually, the damage in the PV fields varies, depending on the category of the defect, from a simple breakdown to a dangerous fire resulting from a defective junction box or poor crimping of connectors that can cause arcing and high heat generation.

Seen the sensitivity of PV systems and in order to avoid the danger caused by the various defects, several failure detection techniques have been developed. Indeed, according to the category of failures, the fault detection techniques for PV system can be grouped as electrical ones, by means of transmittance line diagnosis, I-V tracer for PV monitoring application [1], and time domain reflectometry (TDR) [2], thermal ones are detected by thermography techniques [3], or visual detection, aiming to detect any browning, discoloration, surface soiling and delamination on the PV panels [4]. In the midst of electrical fault detection techniques, TDR and its derivatives, such as the sequence time domain reflectometry (STDR), and spread spectrum time domain reflectometry (SSTDR), have been used for a long time in many different fields, mainly on transmission lines [5] and aircraft wires carrying [6], to detect and locate electrical failures. They proved their effectiveness and reliability for locating such failures either the system to diagnose is on an ON or OFF states. Moreover, their usefulness is not only limited to these applications but also it has been extended to the study of PV systems where the greater seriousness failures like open circuit/Short-circuit [2], ground faults [7], arc faults [8], line-to-line faults [9] were detected and located even in the absence of solar irradiance. However, the TDR and its derivates were used only to detect the final stage of a failure (open-circuit, short-circuit) and neither prevent nor detect a gradual degradation of the PV status, either the deterioration of the connections between panels or inside the panels themselves.

This paper considers TDR as a base for a novel manufacturing defects diagnosis concept, named photovoltaic plant reflectometry profile (PPRP), which represents the reflected signal of a transmitted one within the PV Plant that is compared to the ideal PPRP computed using the datasheet. Unlike previous works, the PPRP allows to find out any change of impedance caused by rust, overheating, corrosion, cable insulation damage or abrasion of connections in the PV array, hence, the PPRP can be used as a gradual fault detection technique and also a predictive tool.

The rest of the paper is organized as follows: Section II presents the TDR concept and the PV module modeling, while Section III describes the novel PPRP concept. Simulation and results are given in Section IV, followed by conclusions in the Section V.

II. Background Concepts

Each PV module is composed by N serial solar cells, where each one is modeled by the well-known equivalent circuit presented in Fig. 1. In fact, the series resistance R_s modelizes three effects: the movement of current through the emitter and base of the solar cell; the contact resistance between the metal contact and the silicon; and finally, the resistance of the top

978-1-5386-4505-5/18/$31.00 ©2018 IEEE

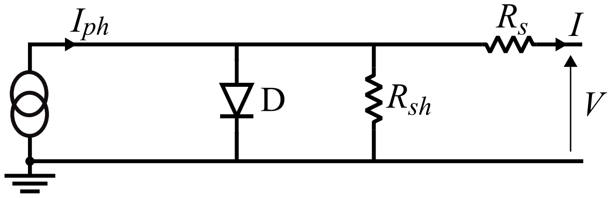

Fig. 1. Equivalent circuit of a solar cell

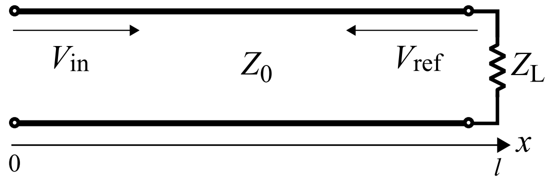

Fig. 2. Simple transmission line model

and rear metal contacts. Similarly, the shunt resistance R_{sh} is due to manufacturing defects, rather than poor solar cell design.

TDR is an electrical fault detection technique usually used for the diagnostic of transmission lines both in telecommunications and electrical distribution network based on sending an incident signal across the transmission line under test which a portion of it will be reflected once it encounters an impedance discontinuity. An oscilloscope is included to monitor the evolution of the signal over time. In Fig. 2, a simple transmission line model is presented, Z_0 is the characteristic impedance of the line and Z_{L} is the load impedance. The reflection coefficient ρ is given by [10],

$$\rho = \frac{Z_{\text{L}} - Z_0}{Z_{\text{L}} + Z_0} = \frac{V_{\text{ref}}}{V_{\text{in}}}, \tag{1}$$

where V_{ref} is the amplitude of the reflected signal and V_{in} is the amplitude of the incident signal. In the case of an impedance mismatch, $Z_{\text{L}} \neq Z_0$, the duration Δt between the incident wave transmission time and the detection of its reflection, is given by,

$$\Delta t = \frac{2l}{v}, \tag{2}$$

where v is the propagation speed, and l is the length of the line.

III. PHOTOVOLTAIC PLANT REFLECTOMETRY PROFILE

Owing to the arduous access to most of PV modules, the detection of defects represents an important diagnostic trouble. In fact, the TDR has been used for long time for the diagnostic of PV plants and it showed that is an efficient technique for both detection and location of PV flaws not only this but it is regarded also as a simple method which neither need a phenomenal devices nor physical access to PV plant sites. Depending to the same basic principle of TDR described above the performance diagnostic of PV plants is realized considering the PV modules as load.

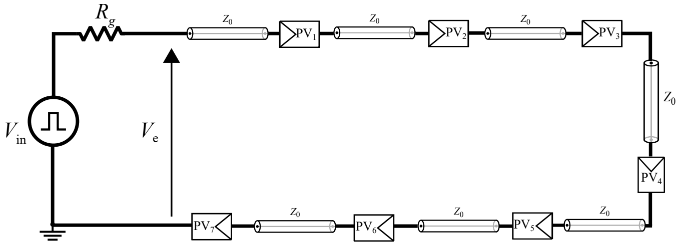

Fig. 3. PV system with seven modules and transmission lines

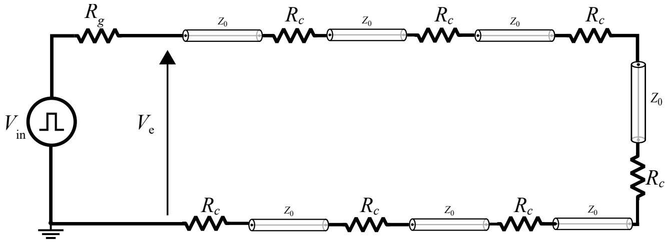

Fig. 4. Equivalent electric schematic of the PV system

A negative pulse signal is transmitted at the output of the PV plant and the reflected signal is recorded in function of time, which represents the measured PPRP. The PPRP is a new analytic model which represents the reflected signal of a transmitted one within the PV Plant that is compared to the ideal (expected) PPRP computed using the datasheet. Indeed, the moment of the change between the two shapes allows the location of the defects by means of (2). The ideal PPRP is considered as the response of a healthy PV system which is used like a baseline for comparison with in the cases of defective PV arrays.

Rather than the known ways in which TDR has always been used and which are limited to the detection of only the first short/open circuit that appears in a photovoltaic field, the PPRP allows on the other hand the detection of any gradual change of impedance which can be caused by: aging, corrosion, wiring mismatch or deterioration of the connections of photovoltaic modules for not only the first occurrence but for the first and all the others that follow it. In addition to all this, the PPRP allowed the validation of the PV modules datasheet once received, instead of testing it one by one and this is realized by the detection of the presence or not of manufacturing defects.

In order to explain the PPRP concept, considers the PV system in Fig. 3 which includes seven PV modules in series intercalated by transmission lines with no solar irradiance (no PV production is available). In addition, a pulse generator provides a negative pulse V_{in} to this PV system through its internal resistance R_{g}. The transmission lines have the same characteristic impedance Z_0 and the same length l.

Indeed, the internal resistance of the pulse generator R_{g} has been chosen in order to maximise the output power of the pulse generator, which means that $R_{\text{g}} = Z_0 = 50\Omega$. Furthermore, due to the negative signal applied to the modules and no-irradiance, the diode (D) of the well-known equivalent circuit

TABLE I
PPRP IN THE CASE OF SEVEN PV MODULES

Time (s)	Voltage $V_e(t)$
$0 \leq t < 2\tau$	βV_{in}
$2\tau \leq t < 4\tau$	$V_{\text{e}[0\leq \text{t}<2\tau]} + \beta V_{\text{in}}\rho_1$
$4\tau \leq t < 6\tau$	$V_{\text{e}[2\tau\leq \text{t}<4\tau]} + \beta V_{\text{in}}(1+\rho_1)^2\alpha^2\rho_1$
$6\tau \leq t < 8\tau$	$V_{\text{e}[4\tau\leq \text{t}<6\tau]} + \beta V_{\text{in}}(1+\rho_1)^4\alpha^4\rho_1 + \beta V_{\text{in}}(1+\rho_1)^2\alpha^2\rho_1^3$
$8\tau \leq t < 10\tau$	$V_{\text{e}[6\tau\leq \text{t}<8\tau]} + \beta V_{\text{in}}(1+\rho_1)^6\alpha^6\rho_1 + 3\beta V_{\text{in}}(1+\rho_1)^4\alpha^4\rho_1^3 + \beta V_{\text{in}}(1+\rho_1)^2\alpha^2\rho_1^5$
$10\tau \leq t < 12\tau$	$V_{\text{e}[8\tau\leq \text{t}<10\tau]} + \beta V_{\text{in}}(1+\rho_1)^8\alpha^8\rho_1 + 6\beta V_{\text{in}}(1+\rho_1)^6\alpha^6\rho_1^3 + 6\beta V_{\text{in}}(1+\rho_1)^4\alpha^4\rho_1^5 + \beta V_{\text{in}}(1+\rho_1)^2\alpha^2\rho_1^7$
$12\tau \leq t < 14\tau$	$V_{\text{e}[10\tau\leq \text{t}<12\tau]} + \beta V_{\text{in}}(1+\rho_1)^{10}\alpha^{10}\rho_1 + 10\beta V_{\text{in}}(1+\rho_1)^8\alpha^8\rho_1^3 + 20\beta V_{\text{in}}(1+\rho_1)^6\alpha^6\rho_1^5 + 10\beta V_{\text{in}}(1+\rho_1)^4\alpha^4\rho_1^7$ $+\beta V_{\text{in}}(1+\rho_1)^2\alpha^2\rho_1^9$
$14\tau \leq t < 16\tau$	$V_{\text{e}[12\tau\leq \text{t}<14\tau]} + \beta V_{\text{in}}(1+\rho_1)^{12}\alpha^{12}\rho_2 + 15\beta V_{\text{in}}(1+\rho_1)^{10}\alpha^{10}\rho_1^3 + 50\beta V_{\text{in}}(1+\rho_1)^8\alpha^8\rho_1^5 + 50\beta V_{\text{in}}(1+\rho_1)^6\alpha^6\rho_1^7$ $+15\beta V_{\text{in}}(1+\rho_1)^4\alpha^4\rho_1^9 + \beta V_{\text{in}}(1+\rho_1)^2\alpha^2\rho_1^{11}$

(Fig. 1) is blocked and this is true for all the solar cells within the PV modules, therefore, each module is equivalent to a resistance R_{c} equal to the sum of N series resistances R_{s} and shunt resistance R_{sh}[1]. Hence, the PV considered model in Fig. 3 is equivalent to the system depicted in Fig. 4, where R_{c}= $N(R_{\text{s}}$+$R_{\text{sh}})$.

Using the transmission line propagation theory [10] and extensive analysis, the ideal (expected) PPRP presented hereafter by the input voltage $V_{\text{e}[2\text{i}\tau\leq\text{t}<2(\text{i}+1)\tau]}$ (Fig. 2) where $i = 0, \ldots, 7$, based on the datasheet, is expressed on Tab. I for the different time intervals $2i\tau \leq t < 2(i+1)\tau$ where $i = 0, \ldots, 7$ and τ is the transmission delay time,

$$\beta = \frac{Z_0}{Z_0 + R_{\text{g}}} = \frac{1}{2}, \tag{3}$$

$$\alpha = \frac{Z_0}{Z_0 + R_{\text{c}}}, \tag{4}$$

$$\rho_1 = \frac{R_{\text{c}}}{2Z_0 + R_{\text{c}}}, \tag{5}$$

and,

$$\rho_2 = \frac{R_{\text{c}} - Z_0}{R_{\text{c}} + Z_0}. \tag{6}$$

IV. SIMULATION AND RESULTS

The standard test conditions (STC) parameters of the PV modules considered in simulations are presented in Tab. II, while the I-V and the P-V curves are presented in Fig. 5. The PPRP profile of a healthy PV plant, which serves as a reference, was done considering the numerical values in Tab. III. The parameters values N, R_{c}, β, α, ρ_1, and ρ_2 are presented in Tab. IV. Based on the mathematical expressions given in Tab. I, the values of the ideal PPRP shape are calculated analytically and presented in Tab. V.

In order to show the ability of the PPRP to detect the gradual defects on the PV modules, two scenarios were simulated. The first one concerns the increase of the resistor value R_{c} of the first PV module PV_1 compared to its normal value, while the second scenario considers the same change but at the third PV module PV_3. Fig. 6 presents the results of the first scenario including both simulations for a healthy and a defective PV plants. The shape of the defective PPRP can be explained as follows:

TABLE II
STC PARAMETERS OF THE TESTED PV MODULE

Parameters	Value
Cell Type	Poly-crystalline 156 × 52 mm
No. of Cells (N)	42 (6 × 7)
Weight	7.0 Kg
Peak Power (Pmax)	50 Wc
Open Circuit Voltage (Voc)	24.8 V
Short Circuit Current (Isc)	2.7 A
Maximum Power Voltage (Vmp)	21 V
Maximum Power Current (Imp)	2.39 A
Shunt Resistor R_{sh}	107.6086
Serial Resistor R_{s}	0.21012
Operating and Storage Temperature	$-40 \sim +85°\text{C}$

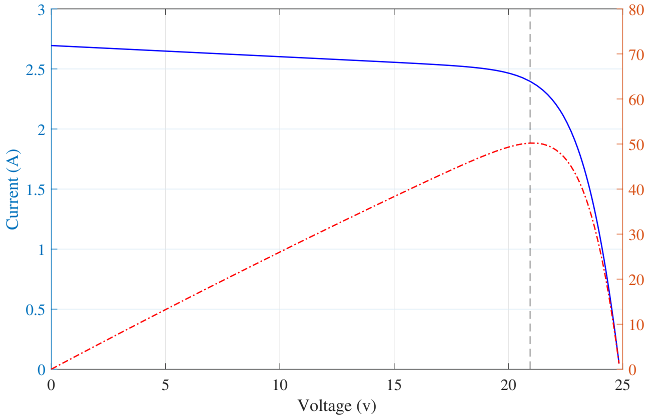

Fig. 5. PV and IV characteristics of the tested PV array

- $t \in [0, 10\text{ns}]$: Within this time interval, both shapes of the ideal and the defective PPRPs are superimposed, because the incident pulse still didn't reach the defective module PV_1.
- After $t = 10$ns: the shapes differ and this is due to the increase of the value R_{c} of the first module PV_1 which is equal to 207.81872Ω instead of its normal value 107.81872Ω. Indeed, the incident signal V_{in} propagates through the PV system, and at $t = \tau = 5$ns, the signal reached the first PV module PV_1, but because Z_0 is

---

[1] R_{s} and R_{sh} can be calculated from the datasheet parameters as indicated in [11].

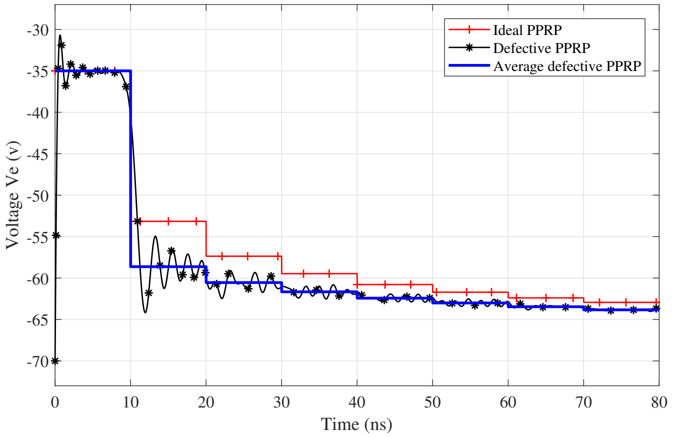

Fig. 6. PPRPs in a scenario with defects on the first PV module

TABLE III
CONSIDERED PARAMETERS VALUES

	Parameters	value
Pulse generator	V_{in}	$-70V$
	Sample time	0.1ns
	R_{g}	50Ω
Transmission line	Z_0	50Ω
	Delay time τ	5ns

different from R_{c} - unmatched line - part of the signal is reflected while the rest of the signal continues to propagate until reaching the seventh PV module PV_7 at $t = 7\tau = 35$ns, which is also an unmatched load. At the end of the transmission lines, the reflected signal is taking $\Delta t = 7\tau = 35$ns to reach the oscilloscope connected at the entrance of the line. At $t = 10$ns, the change in the V_1 value in the defective PPRP shape compared to the ideal one, corresponds to the reflection of the signal at the first PV module PV_1, and is due to impedance changing in the first PV module.

TABLE IV
PARAMETERS VALUES

Parameter	Value
N	42
R_{c}	107.81872Ω
β	0.5
α	0.316819
ρ_1	0.518811
ρ_2	0.366361

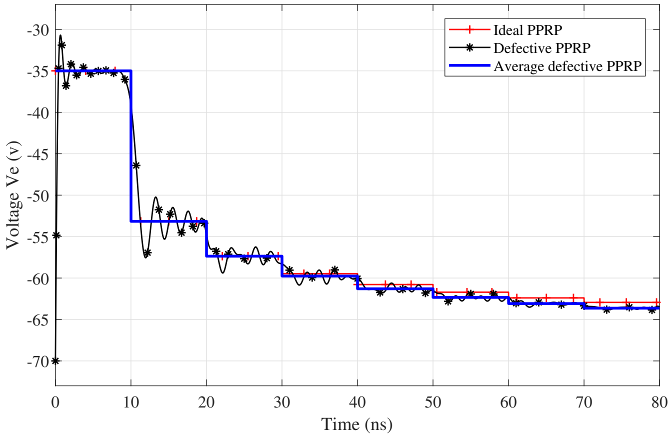

Fig. 7. PPRPs in a scenario with defects on the third PV module

TABLE V
IDEAL PPRP IN THE CASE OF SEVEN SERIAL PV MODULES

Time Intervals	Voltage V_e
$0 \leq t < 2\tau$	-35
$2\tau \leq t < 4\tau$	-53.2
$4\tau \leq t < 6\tau$	-57.4
$6\tau \leq t < 8\tau$	-59.5
$8\tau \leq t < 10\tau$	-60.8
$10\tau \leq t < 12\tau$	-61.7
$12\tau \leq t < 14\tau$	-62.4
$14\tau \leq t < 16\tau$	-62.9

In a second simulation scenario, Fig. 7 presents the PPRP of a defective PV system but at the third PV module PV_3 instead of the first one. In fact, its R_{c} is equal to 207.8186Ω. It is clear from this figure that the shapes of the ideal and the defective PPRPs differ at the instant $t = 30$ns well after the case of defect in PV_1 (scenario 1). The value of the PV module impedance R_{c} in the case of defective systems has been chosen to illustrate the aging, rust, corrosion or any other type of deterioration of the PV module connections. So as a result of those simulations it can be concluded that the concept of the PPRP can pick up any change in the PV array impedance even if it is small, and consequently locate the defective PV module.

V. CONCLUSIONS

This paper presents a new concept called the PPRP which is based on the TDR as a novel technique for the detection and localisation of flaws and defects in a large scale PV array, not only the most known ones like (open circuit, short circuit, line-to-line fault, . . .) but also the smallest change in the impedance of the PV plant generated by rusted, corroded or deteriorated PV modules connections. In addition, it can be also used as a validation tool of the PV modules datasheet rightness of an installed system in one time, instead of testing them one by one.

REFERENCES

[1] C. W. Riley and L. M. Tolbert, "An online autonomous i-v tracer for pv monitoring applications," in *2015 IEEE Power Energy Society General Meeting*, July 2015, pp. 1–5.

[2] L. Schirone, F. P. Califano, and M. Pastena, "Fault detection in a photovoltaic plant by time domain reflectometry," *Progress in Photovoltaics: Research and Applications*, vol. 2, no. 1, pp. 35–44, 1994.

[3] G. S. Spagnolo, P. Del Vecchio, G. Makary, D. Papalillo, and A. Martocchia, "A review of IR thermography applied to PV systems," *2012 11th International Conference on Environment and Electrical Engineering, EEEIC 2012 - Conference Proceedings*, pp. 879–884, 2012.

[4] W. Chine, A. Mellit, V. Lughi, A. Malek, G. Sulligoi, and A. Massi Pavan, “A novel fault diagnosis technique for photovoltaic systems based on artificial neural networks,” *Renewable Energy*, vol. 90, pp. 501–512, 2016.

[5] L. T. Hoai and A. H. Duong, “Fault detection on the transmission lines using the time domain reflectometry method basing on the analysis of reflected waveform,” in *2016 IEEE International Conference on Sustainable Energy Technologies (ICSET)*, Nov. 2016, pp. 241–245.

[6] P. Smith, C. Furse, and J. Gunther, “Analysis of spread spectrum time domain reflectometry for wire fault location,” *IEEE Sensors Journal*, vol. 5, no. 6, pp. 1469–1478, 2005.

[7] M. K. Alam, F. Khan, J. Johnson, and J. Flicker, “PV ground-fault detection using spread spectrum time domain reflectometry (SSTDR),” *2013 IEEE Energy Conversion Congress and Exposition, ECCE 2013*, pp. 1015–1020, 2013.

[8] M. K. Alam, F. H. Khan, J. Johnson, and J. Flicker, “PV arc-fault detection using spread spectrum time domain reflectometry (SSTDR),” *2014 IEEE Energy Conversion Congress and Exposition, ECCE 2014*, pp. 3294–3300, 2014.

[9] M. K. Alam, F. Khan, J. Johnson, and J. Flicker, “A Comprehensive Review of Catastrophic Faults in PV Arrays: Types, Detection, and Mitigation Techniques,” *IEEE Journal of Photovoltaics*, vol. 5, no. 3, pp. 982–997, 2015.

[10] D. Pozar, *Microwave Engineering*, 4th ed., ser. Addison-Wesley series in electrical and computer engineering. Wiley, Dec. 2011.

[11] A. A. E. Tayyan, “Turkish Journal of Physics A simple method to extract the parameters of the single-diode model of a PV system,” *Turk J Phys*, vol. 37, pp. 121–131, 2013.